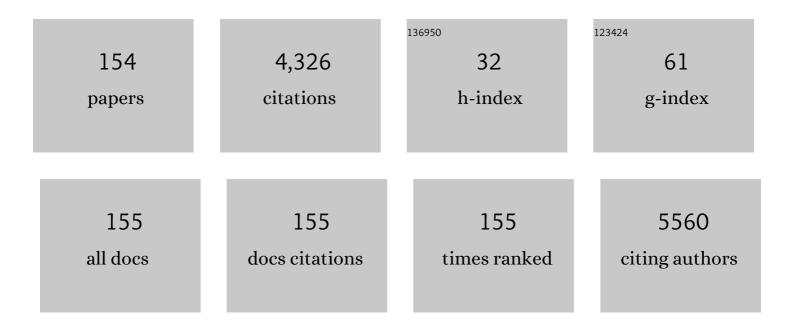
List of Publications by Year in descending order

Source: https://exaly.com/author-pdf/3474927/publications.pdf Version: 2024-02-01



IFONG IN HAN

#	Article	IF	CITATIONS
1	Bi-functional carbon doped and decorated ZnO nanorods for enhanced pH monitoring of dairy milk and adsorption of hazardous dyes. Journal of Industrial and Engineering Chemistry, 2022, , .	5.8	4
2	Flower-like Mo doped Ni(OH)2@Co3S4-Ni3S2 heterostructure for asymmetric supercapacitors. Surfaces and Interfaces, 2022, 30, 101896.	3.0	10
3	Investigating the pseudo – Capacitive properties of interlayer engineered VOPO4 by organic molecule intercalation. Ceramics International, 2022, 48, 26226-26232.	4.8	2
4	In Situ Preparation of Gold–Silica Particles from a Mixture of Oil Palm Leaves and Chloroauric Acid for Reduction of Nitroaromatic Compounds in Water. Waste and Biomass Valorization, 2021, 12, 3773-3780.	3.4	3
5	Induced symmetric 2D Mesoporous Graphitic Carbon Spinel Cobalt Ferrite (CoFe2O4/2D-C) with high porosity fabricated via a facile and swift sucrose templated microwave combustion route for an improved supercapacitive performance. Materials Research Bulletin, 2021, 133, 111053.	5.2	7
6	Robust structural stability and performanceâ€enhanced asymmetric supercapacitors based on CuMoO4/ZnMoO4 nanoflowers prepared via a simple and low-energy precipitation route. Journal of Materials Science: Materials in Electronics, 2021, 32, 6668-6681.	2.2	14
7	Potentiometric Performance of a Highly Flexible-Shaped Trifunctional Sensor Based on ZnO/V2O5 Microrods. Sensors, 2021, 21, 2559.	3.8	4
8	Construction of NiCo-OH/Ni3S2 core-shell heterostructure wrapped in rGO nanosheets as efficient supercapacitor electrode enabling high stability up to 20,000 cycles. Journal of Electroanalytical Chemistry, 2021, 889, 115226.	3.8	12
9	Flexible and patterned-free Ni/NiO-based temperature device on cylindrical PET fabricated by RF magnetron sputtering: Bending and washing endurance tests. Journal of Industrial and Engineering Chemistry, 2021, 100, 372-382.	5.8	8
10	One-pot synthesis of ultrahigh performance nanorod structured Co3O4@Fe2O3 anchored on a resonating 2D-carbon with high potential window and surface area for supercapacitors application. Ceramics International, 2021, 47, 23665-23669.	4.8	4
11	Reinforced supercapacitive behavior of O3-type layer-structured Na3Ni2BiO6 in 1-butyl-3-methylimidazolium tetrafluoroborate (BMIMBF4) electrolyte. Journal of Materials Science: Materials in Electronics, 2020, 31, 16688-16700.	2.2	2
12	Biogenesis of Prism-Like Silver Oxide Nanoparticles Using Nappa Cabbage Extract and Their p-Nitrophenol Sensing Activity. Molecules, 2020, 25, 2298.	3.8	6
13	Newly Design Porous/Sponge Red Phosphorus@Graphene and Highly Conductive Ni2P Electrode for Asymmetric Solid State Supercapacitive Device With Excellent Performance. Nano-Micro Letters, 2020, 12, 25.	27.0	44
14	Quaternary transition metal molybdate (Mn 0.25Ni0.25Co0.25Fe0.25MoO4) design to improve the kinetics of the redox reaction in supercapacitors. Ceramics International, 2020, 46, 12422-12429.	4.8	14
15	Development of a Highly Flexible and Durable Fiber-Shaped Temperature Sensor Based on Graphene/Ni Double-Decked Layer for Wearable Devices. IEEE Sensors Journal, 2020, 20, 5146-5154.	4.7	12
16	Sucrose-templated interconnected meso/macro-porous 2D symmetric graphitic carbon networks as supports for α-Fe ₂ O ₃ towards improved supercapacitive behavior. RSC Advances, 2020, 10, 15751-15762.	3.6	4
17	Development of flexible, stable, and efficient inverted organic solar cells harvesting light in all directions. Electrochimica Acta, 2019, 326, 134985.	5.2	3
18	Preparation of hierarchical flower-like nickel sulfide as hole transporting material for organic solar cells via a one-step solvothermal method. Solar Energy, 2019, 188, 403-413.	6.1	12

#	Article	IF	CITATIONS
19	Polypyrrole nanostructures//activated carbon based electrode for energy storage applications. Journal of Materials Science: Materials in Electronics, 2019, 30, 7890-7900.	2.2	5
20	Enhancing the photovoltaic characteristics of organic solar cells by introducing highly conductive graphene as a conductive platform for a PEDOT:PSS anode interfacial layer. Journal of Materials Science: Materials in Electronics, 2019, 30, 6187-6200.	2.2	15
21	Enhanced pseudocapacitance of NiSe2/Ni(OH)2 nanocomposites for supercapacitor electrode. Materials Letters, 2019, 234, 87-91.	2.6	28
22	Studies on the graded band-gap copper indium di-selenide thin film solar cells prepared by electrochemical route. Applied Surface Science, 2019, 466, 358-366.	6.1	7
23	Robust cyclic stability and high-rate asymmetric supercapacitor based on orange peel-derived nitrogen-doped porous carbon and intercrossed interlinked urchin-like NiCo2O4@3DNF framework. Electrochimica Acta, 2019, 293, 84-96.	5.2	62
24	Significant improvement in the photovoltaic stability of bulk heterojunction organic solar cells by the molecular level interaction of graphene oxide with a PEDOT: PSS composite hole transport layer. Solar Energy, 2018, 167, 24-34.	6.1	41
25	Facilely synthesized NiMoO4/CoMoO4 nanorods as electrode material for high performance supercapacitor. Journal of Alloys and Compounds, 2018, 742, 342-350.	5.5	119
26	Facile room temperature synthesis and application of MnMoO4·0.9H2O as supercapacitor electrode material. Materials Letters, 2018, 217, 146-150.	2.6	25
27	Fabrication of highly flexible conducting electrode based on MnS nanoparticles/graphite/scotch tape for supercapacitor applications. Journal of Materials Science: Materials in Electronics, 2018, 29, 1636-1642.	2.2	13
28	Facile synthesis of ZnS/MnS nanocomposites for supercapacitor applications. Journal of Solid State Electrochemistry, 2018, 22, 303-313.	2.5	69
29	Single fiber UV detector based on hydrothermally synthesized ZnO nanorods for wearable computing devices. Applied Surface Science, 2018, 428, 233-241.	6.1	29
30	Fabrication of β-Ni(OH)2Ââ^¥Âγ-Fe2O3 nanostructures for high-performance asymmetric supercapacitors. Journal of Solid State Electrochemistry, 2018, 22, 293-302.	2.5	8
31	Interface engineering of G-PEDOT: PSS hole transport layer via interlayer chemical functionalization for enhanced efficiency of large-area hybrid solar cells and their charge transport investigation. Solar Energy, 2018, 174, 743-756.	6.1	23
32	Improving the conductivity of PEDOT:PSS to nearly 1 million S/m with graphene on an ITO-glass substrate. Synthetic Metals, 2018, 245, 276-285.	3.9	21
33	Study of interface chemistry between the carrier-transporting layers and their influences on the stability and performance of organic solar cells. Applied Nanoscience (Switzerland), 2018, 8, 1325-1341.	3.1	9
34	Solid State Supercapacitor Based on Manganese Oxide@Reduced Graphene Oxide and Polypyrrole Electrodes. ChemElectroChem, 2018, 5, 2747-2757.	3.4	17
35	The effect of the functionalization of multiple carrier transporting interlayers on the performance and stability of bulk heterojunction organic solar cells. Journal of Materials Science: Materials in Electronics, 2018, 29, 13561-13576.	2.2	3
36	Electrical structure, magnetic polaron and lithium ion dynamics in four mixed-metal oxide multiple-phase electrode cathode material for Li ion batteries from density functional theory study. Computational Materials Science, 2017, 132, 92-103.	3.0	9

#	Article	IF	CITATIONS
37	High Performance Cylindrical Capacitor as a Relative Humidity Sensor for Wearable Computing Devices. Journal of the Electrochemical Society, 2017, 164, B136-B141.	2.9	18
38	Honeycomb layered oxide Na3Ni2SbO6 for high performance pseudocapacitor. Journal of Alloys and Compounds, 2017, 704, 734-741.	5.5	16
39	The effect of the nickel and chromium concentration ratio on the temperature coefficient of the resistance of a Ni–Cr thin film-based temperature sensor. Sensors and Actuators A: Physical, 2017, 260, 198-205.	4.1	16
40	Cylindrical relative humidity sensor based on poly-vinyl alcohol (PVA) for wearable computing devices with enhanced sensitivity. Sensors and Actuators A: Physical, 2017, 261, 268-273.	4.1	34
41	Resistive behavior of Ni thin film on a cylindrical PET monofilament with temperature for wearable computing devices. Sensors and Actuators A: Physical, 2017, 259, 96-104.	4.1	10
42	Layered Na2/3Ni1/3Mn2/3O2 as electrode material with two redox active transition metals for high performance supercapacitor. Journal of Alloys and Compounds, 2017, 728, 78-87.	5.5	11
43	Fabrication of thermally evaporated Al thin film on cylindrical PET monofilament for wearable computing devices. Electronic Materials Letters, 2016, 12, 186-196.	2.2	10
44	Electrical Properties of Conductive Cotton Yarn Coated with Eosin Y Functionalized Reduced Graphene Oxide. Journal of Nanoscience and Nanotechnology, 2016, 16, 6061-6067.	0.9	5
45	Electrical structures, magnetic polaron and lithium ion dynamics in three transition metal doped LiFe1â^'xMxPO4 (M = Mn, Co and La) cathode material for Li ion batteries from density functional theory study. Solid State Ionics, 2016, 294, 73-81.	2.7	16
46	Synthesis, characterization and lithium-ion migration dynamics simulation of LiFe1â"x T x PO4 (TÂ=ÂMn,) Tj ET and Processing, 2016, 122, 1.	Qq0 0 0 rgl 2.3	BT /Overlock I 8
47	Facile hydrothermal synthesis of hexapod-like two dimensional dichalcogenide NiSe2 for supercapacitor. Materials Letters, 2016, 181, 345-349.	2.6	92
48	Size effect on negative capacitance at forward bias in InGaN/GaN multiple quantum well-based blue LED. Electronic Materials Letters, 2016, 12, 67-75.	2.2	14
49	Electrical characterization and thermal admittance spectroscopy analysis of InGaN/GaN MQW blue LED structure. Electronic Materials Letters, 2015, 11, 982-992.	2.2	23
50	Synthesis and characterization of α-Fe2O3 Micro-/Nanorods-modified glassy carbon electrode for electrochemical sensing of nitrobenzene. Ceramics International, 2015, 41, 5568-5573.	4.8	31
51	Photocatalytic degradation of acid orange 7 using Cr-doped CeO2 nanorods. Journal of Materials Science: Materials in Electronics, 2015, 26, 1441-1448.	2.2	8
52	Enhanced photocatalytic property of self-assembled Fe-doped CeO2 hierarchical nanostructures. Materials Letters, 2015, 145, 189-192.	2.6	35
53	Fabrication of CeO ₂ /Fe ₂ O ₃ composite nanospindles for enhanced visible light driven photocatalysts and supercapacitor electrodes. Journal of Materials Chemistry A, 2015, 3, 15248-15258.	10.3	189
54	Effect of SiO2 nanoparticle doping on electro-optical properties of polymer dispersed liquid crystal lens for smart electronic glasses. Nano Convergence, 2015, 2, .	12.1	18

#	Article	IF	CITATIONS
55	Facile hydrothermal synthesis of CeO2 nanopebbles. Bulletin of Materials Science, 2015, 38, 1135-1139.	1.7	14
56	Structure and electrochemical detection of xenobiotic micro-pollutant hydroquinone using CeO ₂ nanocrystals. RSC Advances, 2015, 5, 70558-70565.	3.6	11
57	Electroless plating of copper nanoparticles on PET fiber for non-enzymatic electrochemical detection of H ₂ O ₂ . RSC Advances, 2015, 5, 76729-76732.	3.6	13
58	Solution-processed indium–tin-oxide nanoparticle transparent conductors on flexible glass substrate with high optical transmittance and high thermal stability. Japanese Journal of Applied Physics, 2014, 53, 08NF04.	1.5	5
59	Solvothermal synthesis of threeâ€dimensional CeO ₂ micropillows and their photocatalytic property. Physica Status Solidi - Rapid Research Letters, 2014, 8, 643-647.	2.4	3
60	Effect of cell gap on electro-optical properties of polymer dispersed liquid crystal lens for smart electronic glasses. Electronic Materials Letters, 2014, 10, 857-861.	2.2	12
61	Effect of liquid crystal concentration on electro-optical properties of polymer dispersed liquid crystal lens for smart electronic glasses with auto-shading and auto-focusing function. Electronic Materials Letters, 2014, 10, 607-610.	2.2	17
62	Effect of UV intensity on the electro-optical properties of polymer dispersed liquid crystal lens for smart electronic glasses. Electronic Materials Letters, 2014, 10, 665-669.	2.2	13
63	Effects of oxide electron transport layer on quantum dots light emitting diode with an organic/inorganic hybrid structure. Electronic Materials Letters, 2013, 9, 779-782.	2.2	9
64	IR Sensor Synchronizing Active Shutter Glasses for 3D HDTV with Flexible Liquid Crystal Lenses. Sensors, 2013, 13, 16583-16590.	3.8	4
65	High-Performance 2,8-Difluoro-5,11-bis(triethylsilylethynyl) Anthradithiophene Thin-Film Transistors Facilitated by Predeposited Ink-Jet Blending. Japanese Journal of Applied Physics, 2013, 52, 031601.	1.5	5
66	Active shutter glasses for 3D HDTV with flexible liquid crystal lens. , 2013, , .		1
67	Enhanced Stability of All Solution-Processed Organic Thin-Film Transistors Using Highly Conductive Modified Polymer Electrodes. Japanese Journal of Applied Physics, 2012, 51, 091602.	1.5	2
68	High-Performance Semitransparent Bulk-Heterojunction Organic Photovoltaics with Ag Interfacial Layer. Japanese Journal of Applied Physics, 2012, 51, 024104.	1.5	0
69	Effect of Zinc/Tin Composition Ratio on the Operational Stability of Solution-Processed Zinc–Tin–Oxide Thin-Film Transistors. IEEE Electron Device Letters, 2012, 33, 50-52.	3.9	57
70	Improvement of electrical properties of printed ITO thin films by heat-treatment conditions. Current Applied Physics, 2011, 11, S202-S205.	2.4	13
71	Fast and Stable Solution-Processed Transparent Oxide Thin-Film Transistor Circuits. IEEE Electron Device Letters, 2011, 32, 524-526.	3.9	22
72	Improving the Electrical Properties of Zinc Tin Oxide Thin Film Transistors Using Atmospheric Plasma Treatment. Electrochemical and Solid-State Letters, 2011, 14, H354.	2.2	10

#	Article	IF	CITATIONS
73	Transparent organic light-emitting devices with CsCl capping layers on semitransparent Ca/Ag cathodes. Materials Science and Engineering B: Solid-State Materials for Advanced Technology, 2010, 172, 76-79.	3.5	10
74	Effect of Metallic Composition on Electrical Properties of Solution-Processed Indium-Gallium-Zinc-Oxide Thin-Film Transistors. IEEE Transactions on Electron Devices, 2010, 57, 1009-1014.	3.0	69
75	Highly light-responsive ink-jet printed 6,13-bis(triisopropylsilylethynyl) pentacene phototransistors with suspended top-contact structure. Organic Electronics, 2010, 11, 1529-1533.	2.6	30
76	Top emission organic light-emitting devices with CsCl capping layer. Thin Solid Films, 2010, 518, 2793-2795.	1.8	3
77	Eco-friendly synthesis of SiO2 nanoparticles with high purity for digital printing. Thin Solid Films, 2010, 518, 6634-6637.	1.8	2
78	Solvent-mediated threshold voltage shift in solution-processed transparent oxide thin-film transistors. Applied Physics Letters, 2010, 97, 092105.	3.3	14
79	Coupling Top- and Bottom-Gate ZnO Thin Film Transistors for Low Voltage, High Gain Inverter. Electrochemical and Solid-State Letters, 2010, 13, H194.	2.2	5
80	Physical and Electrical Properties of SiO2Layer Synthesized by Eco-Friendly Method. Japanese Journal of Applied Physics, 2010, 49, 05EA02.	1.5	4
81	Ink-Jet-Printed Zinc–Tin–Oxide Thin-Film Transistors and Circuits With Rapid Thermal Annealing Process. IEEE Electron Device Letters, 2010, 31, 836-838.	3.9	45
82	Effects of the Concentration of Indium-tin-oxide (ITO) Ink on the Characteristics of Directly-printed ITO Thin Films. Journal of the Korean Physical Society, 2010, 57, 1794-1798.	0.7	7
83	All solution-processed high-resolution bottom-contact transparent metal-oxide thin film transistors. Journal Physics D: Applied Physics, 2009, 42, 125102.	2.8	53
84	Effect of Annealing Treatment and Surface Morphology on Power Conversion in Organic Photovoltaics. Japanese Journal of Applied Physics, 2009, 48, 081505.	1.5	9
85	Sr/Ag semitransparent cathodes for top emission organic light-emitting devices. Thin Solid Films, 2009, 517, 2035-2038.	1.8	5
86	Environmental and operational stability of solution-processed 6,13-bis(triisopropyl-silylethynyl) pentacene thin film transistors. Organic Electronics, 2009, 10, 486-490.	2.6	77
87	High-resolution patterned nanoparticulate Ag electrodes toward all printed organic thin film transistors. Organic Electronics, 2009, 10, 1102-1108.	2.6	25
88	Color Stability of White Organic Light Emitting Diodes as Position of Partially Doped Rubrene in DPVBi Emission Layer. Molecular Crystals and Liquid Crystals, 2009, 499, 66/[388]-74/[396].	0.9	0
89	High Performance Solution-Processed and Lithographically Patterned Zinc–Tin Oxide Thin-Film Transistors with Good Operational Stability. Electrochemical and Solid-State Letters, 2009, 12, H256.	2.2	72
90	Characteristics of ITO and Overcoat Layer for Full Color Organic Light Emitting Diode with Color Filter. Molecular Crystals and Liquid Crystals, 2009, 499, 58/[380]-65/[387].	0.9	0

#	Article	IF	CITATIONS
91	Glycerol-Doped Poly(3,4-ethylenedioxy-thiophene):Poly(styrene sulfonate) Buffer Layer for Improved Power Conversion in Organic Photovoltaic Devices. Journal of the Electrochemical Society, 2009, 156, H782.	2.9	22
92	Roomâ€Temperature Selfâ€Organizing Characteristics of Soluble Acene Fieldâ€Effect Transistors. Advanced Functional Materials, 2008, 18, 560-565.	14.9	40
93	Development of Ultrafine Indium Tin Oxide (ITO) Nanoparticle for Ink-Jet Printing by Low-Temperature Synthetic Method. IEEE Nanotechnology Magazine, 2008, 7, 172-176.	2.0	53
94	Dynamic Characteristics of Vertically Aligned Liquid Crystal Device Using a Polymer Wall Associated with the Boundary Condition of Alignment Layer. Molecular Crystals and Liquid Crystals, 2007, 476, 115/[361]-123/[369].	0.9	0
95	Hybrid Passivation for a Film-like Organic Light-Emitting Diode using Parylene and Silicon Dioxide. Japanese Journal of Applied Physics, 2007, 46, 810-814.	1.5	7
96	Solution-processable pentacene microcrystal arrays for high performance organic field-effect transistors. Applied Physics Letters, 2007, 90, 132106.	3.3	140
97	Organic thin-film transistors using suspended source/drain electrode structure. Applied Physics Letters, 2007, 91, 042113.	3.3	7
98	Spiro-silacycloalkyl Tetraphenylsiloles with a Tunable Exocyclic Ring:Â Preparation, Characterization, and Device Application of 1,1â€~-Silacycloalkyl-2,3,4,5-tetraphenylsiloles. Organometallics, 2007, 26, 519-526.	2.3	36
99	Fabrication of low-temperature-polysilicon thin-film transistors on flexible substrates using excimer-laser crystallization. Journal of the Society for Information Display, 2007, 15, 1105.	2.1	2
100	High-Mobility Organic Transistors Based on Single-Crystalline Microribbons of Triisopropylsilylethynyl Pentacene via Solution-Phase Self-Assembly. Advanced Materials, 2007, 19, 678-682.	21.0	339
101	Effect of synthetic conditions on particle size and photo-luminescence properties of Y2O3:Eu3+ nanophosphor. Journal of Electroceramics, 2007, 18, 67-71.	2.0	5
102	Ca/Ag bilayer cathode for transparent white organic light-emitting devices. Applied Surface Science, 2007, 253, 4249-4253.	6.1	23
103	Green top-emitting organic light emitting device with transparent Baâ^•Ag bilayer cathode. Applied Physics Letters, 2006, 89, 123501.	3.3	18
104	Influence of Eu3+ doping content on photoluminescence of Gd2O3:Eu3+ phosphors prepared by liquid-phase reaction method. Journal of Luminescence, 2006, 118, 199-204.	3.1	27
105	Synthesis and characterization of indium tin oxide (ITO) nanoparticle using gas evaporation process. Journal of Electroceramics, 2006, 17, 821-826.	2.0	15
106	Effects of parylene buffer layer on flexible substrate in organic light emitting diode. Thin Solid Films, 2006, 513, 258-263.	1.8	39
107	Transparent White OLEDs Using Ca-Ag Cathode. Molecular Crystals and Liquid Crystals, 2006, 459, 75/[355]-84/[364].	0.9	0
108	Red electrophosphorescent top emission organic light-emitting device with Caâ^•Ag semitransparent cathode. Applied Physics Letters, 2006, 89, 253508.	3.3	16

#	Article	IF	CITATIONS
109	Fabrication of 5,6,11,12 -tetraphenyl-naphthacene doped 4-bis(2,2-diphenylvinyl)-1,1-biphenyl white organic light-emitting device. Applied Physics Letters, 2006, 89, 223514.	3.3	0
110	Efficient red electrophosphorescent top-emitting organic light-emitting devices. Materials Science and Engineering B: Solid-State Materials for Advanced Technology, 2005, 121, 232-237.	3.5	11
111	Enhancement of Field-Effect Mobility Due to Surface-Mediated Molecular Ordering in Regioregular Polythiophene Thin Film Transistors. Advanced Functional Materials, 2005, 15, 77-82.	14.9	441
112	Thermal Behavior of SnO2–5 wt % Pd Composite Nanoparticles Fabricated byIn-SituSynthetic Method. Japanese Journal of Applied Physics, 2005, 44, 7698-7702.	1.5	6
113	Color Tracking Analysis of the Fringe-Field-Switching Cell Using a Liquid Crystal with Negative Dielectric Anisotropy. Japanese Journal of Applied Physics, 2005, 44, 225-228.	1.5	2
114	Low-temperature catalyst adding for tin-oxide nanostructure gas sensors. IEEE Sensors Journal, 2005, 5, 12-19.	4.7	6
115	Organic thin-film devices on paper substrates. Journal of the Society for Information Display, 2005, 13, 829.	2.1	10
116	Position Dependent Stress Distribution of Indium-Tin-Oxide on Polymer Substrate by Applying External Bending Force. Japanese Journal of Applied Physics, 2004, 43, 2677-2680.	1.5	3
117	Transient electrophosphorescence in red top-emitting organic light-emitting devices. Applied Physics Letters, 2004, 85, 4771-4773.	3.3	16
118	Organic Thin Film Transistor-Driven Liquid Crystal Displays on Flexible Polymer Substrate. Japanese Journal of Applied Physics, 2004, 43, 3605-3608.	1.5	24
119	Control of High Pretilt Angle for Nematic Liquid Crystal on Homeotropic Alignment Layer by In-situ Photoalignment Method. Molecular Crystals and Liquid Crystals, 2004, 412, 269-275.	0.9	6
120	Organic TFT Array on a Paper Substrate. IEEE Electron Device Letters, 2004, 25, 702-704.	3.9	160
121	Resistivity Characteristics of Plastic Multi-Barrier ITO Film by the Bending Process. Ferroelectrics, 2004, 303, 155-158.	0.6	0
122	Active-matrix liquid crystal display using solution-based organic thin film transistors on plastic substrates. Displays, 2004, 25, 167-170.	3.7	24
123	Realization of an efficient top emission organic light-emitting device with novel electrodes. Thin Solid Films, 2004, 467, 201-208.	1.8	45
124	Effect of low temperature composite catalyst loading (LTC2L) on sensing properties of nano gas sensor. Sensors and Actuators A: Physical, 2004, 112, 80-86.	4.1	7
125	Transparent conducting metal electrode for top emission organic light-emitting devices: Ca–Ag double layer. Applied Physics Letters, 2004, 84, 4614-4616.	3.3	138
126	Failure of the top emission organic light-emitting device with a Ca/Ag semitransparent cathode. Synthetic Metals, 2004, 146, 63-68.	3.9	14

#	Article	IF	CITATIONS
127	Electrical and mechanical properties of low temperature evaporated silicon dioxide/polyimide dual-layer insulator for plastic-based polymer transistor. Thin Solid Films, 2003, 429, 231-237.	1.8	16
128	Admittance Spectroscopic Characteristics and Equivalent Circuit Modeling of Small Molecule-Based Organic Light Emitting Diodes. Japanese Journal of Applied Physics, 2003, 42, 2715-2718.	1.5	12
129	Electrical characteristics of poly (3-hexylthiophene) thin film transistors printed and spin-coated on plastic substrates. Synthetic Metals, 2003, 139, 377-384.	3.9	42
130	Improvement of luminance efficiency in xenon dielectric barrier discharge flat lamp. IEEE Transactions on Plasma Science, 2003, 31, 176-179.	1.3	10
131	Mechanical Stability of Externally Deformed Indium–Tin–Oxide Films on Polymer Substrates. Japanese Journal of Applied Physics, 2003, 42, 623-629.	1.5	115
132	Electro-Mechanical Properties of Metal–Insulator–Metal Device Fabricated on Polymer Substrate Using Low-Temperature Process. Japanese Journal of Applied Physics, 2002, 41, 533-540.	1.5	6
133	High Performance Polymer Thin Film Transistors Array Printed on a Flexible Polycarbonate Substrate. Materials Research Society Symposia Proceedings, 2002, 736, 1.	0.1	6
134	Electro-structural and Film Growth Properties of Room-temperature Deposited Indium-Tin-Oxide on Polymer Substrates. Materials Research Society Symposia Proceedings, 2002, 747, 1.	0.1	0
135	High-performance polymer tfts printed on a plastic substrate. IEEE Transactions on Electron Devices, 2002, 49, 2008-2015.	3.0	60
136	Flexible metal–insulator–metal (MIM) devices for plastic film AM-LCD. Current Applied Physics, 2002, 2, 245-248.	2.4	11
137	Analysis of ITO Films Deposited on Various Polymer Substrates for High-Resolution Plastic Film LCDs. Materials Research Society Symposia Proceedings, 2001, 685, 1.	0.1	3
138	Mechanics of Indium-Tin-Oxide Films on Polymer Substrates with Organic Buffer Layer. Materials Research Society Symposia Proceedings, 2001, 695, 1.	0.1	1
139	Electrical and mechanical properties of indiumâ€ŧinâ€oxide films deposited on polymer substrate using organic buffer layer. Journal of Information Display, 2001, 2, 52-60.	4.0	4
140	Deposition of indium–tin-oxide films on polymer substrates for application in plastic-based flat panel displays. Thin Solid Films, 2001, 397, 49-55.	1.8	185
141	Chip Bonding on Non-rigid and Flexible Substrates with New Stepped Processes. Japanese Journal of Applied Physics, 2001, 40, 412-418.	1.5	14
142	Glass-to-glass electrostatic bonding for FED tubeless packaging application. Microelectronics Journal, 1998, 29, 839-844.	2.0	2
143	Time-resolved spectroscopic study of energy transfer in ZnO:EuCl3 phosphors. Journal of Luminescence, 1998, 78, 87-90.	3.1	51
144	Effect of coupling structure of Eu on the photoluminescent characteristics for ZnO:EuCl3 phosphors. Applied Physics Letters, 1998, 72, 668-670.	3.3	51

#	Article	IF	CITATIONS
145	Experimental and theoretical considerations on evacuation of vacuum package for field emission display. Journal of Vacuum Science & Technology an Official Journal of the American Vacuum Society B, Microelectronics Processing and Phenomena, 1998, 16, 1236.	1.6	13
146	Growth and luminescent characteristics of ZnGa[sub 2]O[sub 4] thin film phosphor prepared by radio frequency magnetron sputtering. Journal of Vacuum Science & Technology an Official Journal of the American Vacuum Society B, Microelectronics Processing and Phenomena, 1998, 16, 1239.	1.6	13
147	Ni Electroless Plating Process for Solder Bump Chip on Glass Technology. Japanese Journal of Applied Physics, 1997, 36, 2091-2095.	1.5	9
148	Simulation of the degradation behavior of the hydrogen absorption kinetics of LaNi5 under the cyclic operations in H2-CO and H2-O2. Journal of the Less Common Metals, 1990, 157, 187-199.	0.8	6
149	Hydriding kinetics of LaNi5 and LaNi4.7Al0.3. International Journal of Hydrogen Energy, 1989, 14, 181-186.	7.1	20
150	The effect of CO impurity on the hydrogenation properties of LaNi5, LaNi4.7Al0.3 and MmNi4.5Al0.5 during hydriding-dehydriding cycling. Journal of the Less Common Metals, 1989, 152, 319-327.	0.8	19
151	Influence of oxygen impurity on the hydrogenation properties of LaNi5, LaNi4.7Al0.3 and MmNi4.5Al0.5 during long-term pressure-induced hydriding-dehydriding cycling. Journal of the Less Common Metals, 1989, 152, 329-338.	0.8	28
152	Thermal Desorption Study of LaNi5 Degraded by Pressure Cycling*. Zeitschrift Fur Physikalische Chemie, 1989, 164, 1291-1292.	2.8	2
153	An investigation of the intrinsic degradation mechanism of LaNi5 by thermal desorption technique. International Journal of Hydrogen Energy, 1988, 13, 577-581.	7.1	30
154	Effect of substitution of titanium by zirconium in TiFe on hydrogenation properties. Journal of the Less Common Metals, 1986, 119, 237-246.	0.8	32